SCALER: SAM-Enhanced Collaborative Learning for Label-Deficient Concealed Object Segmentation

Chunming He¹, Rihan Zhang¹, Longxiang Tang², Ziyun Yang³, Kai Li⁴, Deng-Ping Fan⁵, and Sina Farsiu^{1,†}

¹Duke University, ²Harvard University, ³Apple, ⁴Meta, ⁵Nankai University, [†] Corresponding Author, Contact: chunming.he@duke.edu.

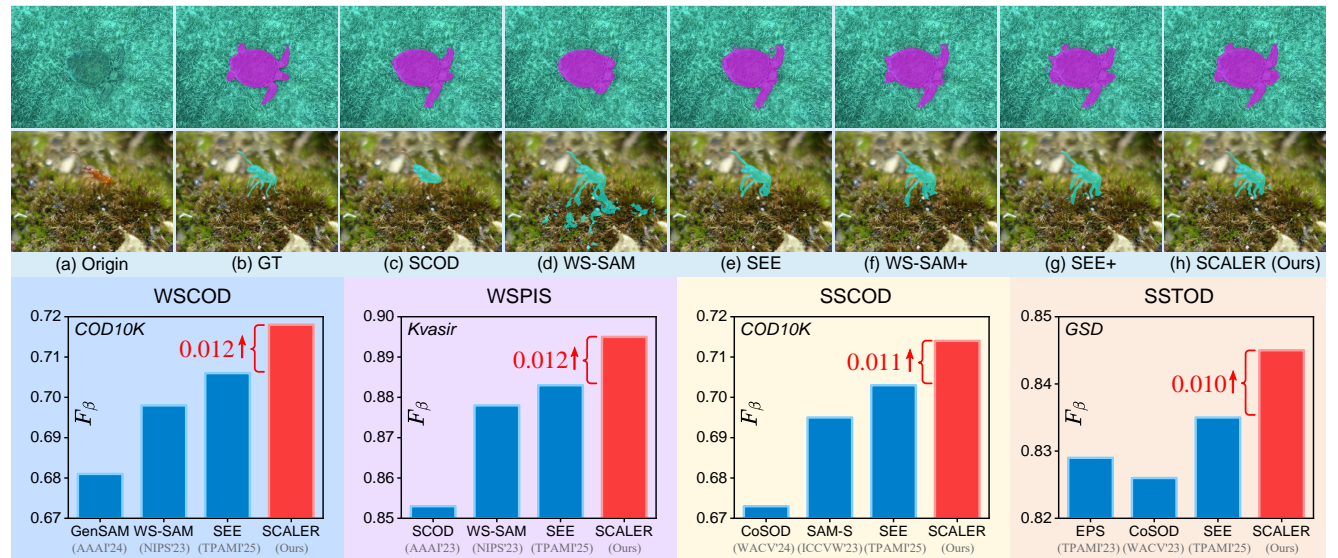


Figure 1. Results of existing LDCOS methods with point supervision, including SCOD [15], WS-SAM [11], and SEE [13]. The suffix "+" denotes integration with SCALER. SCALER yields more accurate concealed-object segmentation and achieves leading results across COD (camouflaged object detection), PIS (polyp image segmentation), and TOD (transparent object detection) under weak (WS) and semi-supervised (SS) settings. In the top section, concealed objects masks are highlighted in pink and blue.

Abstract

Existing methods for label-deficient concealed object segmentation (LDCOS) either rely on consistency constraints or Segment Anything Model (SAM)-based pseudo-labeling. However, their performance remains limited due to the intrinsic concealment of targets and the scarcity of annotations. This study investigates two key questions: (1) Can consistency constraints and SAM-based supervision be jointly integrated to better exploit complementary information and enhance the segmenter? and (2) beyond that, can the segmenter in turn guide SAM through reciprocal supervision, enabling mutual improvement? To answer these questions, we present SCALER, a unified collaborative framework toward LDCOS that jointly optimizes a mean-teacher segmenter and a learnable SAM. SCALER operates in two alternating phases. In **Phase I**, the segmenter is optimized under fixed SAM supervision using entropy-based image-level and uncertainty-based pixel-level weighting to select reliable

pseudo-label regions and emphasize harder examples. In **Phase II**, SAM is updated via augmentation invariance and noise resistance losses, leveraging its inherent robustness to perturbations. Experiments demonstrate that SCALER yields consistent performance gains across eight semi- and weakly-supervised COS tasks. The results further suggest that SCALER can serve as a general training paradigm to enhance both lightweight segmenters and large foundation models under label-scarce conditions. Code will be released.

1. Introduction

Concealed object segmentation (COS) encompasses scenarios where targets share high visual similarity with their surroundings, making them difficult to distinguish. Representative tasks include camouflaged object detection (COD) [6, 10], polyp image segmentation (PIS) [7, 27], medical tubular object segmentation (MTOS) [9, 14], and transparent object detection (TOD) [11, 28]. Unlike conventional

segmentation, COS must contend with weak contrast and ambiguous boundaries, which significantly complicate training. Early studies mitigated these difficulties through perceptual priors [12, 31] and auxiliary cues [10, 25], showing strong results under full supervision.

The challenge grows sharper in label-deficient COS (LD-COS), including semi- (SSCOS) and weakly-supervised (WSCOS) setups, where limited annotations constrain learning. Prior works have extended consistency-based frameworks, particularly the mean-teacher paradigm that enforces prediction stability between a student and an exponentially averaged teacher [15, 20]. However, the reliance on pseudolabels often introduces error accumulation, especially for concealed targets with uncertain boundaries (see Fig. 1).

To exploit foundation model guidance, recent works such as WS-SAM[11] and SEE[13] employed the pretrained Segment Anything Model (SAM)[19] as an external teacher, transferring its global knowledge to task-specific segmenters. These methods confirm SAM's potential in providing supplementary supervision, yet face two major limitations (see Fig. 2). First, SAM's fixed predictions are not tailored for COS, yielding noisy and suboptimal pseudo labels. Second, the information flow remains one-way, from SAM to the segmenter, without allowing the evolving, task-adapted segmenter to reciprocally benefit SAM.

These shortcomings raise two central questions: (1) Can consistency learning and SAM-based supervision be jointly leveraged to improve segmenters under label scarcity? (2) Can the segmenter itself provide pseudo-label feedback to strengthen SAM, enabling mutual improvement?

To address these questions, we propose **SCALER**, a SAM-enhanced collaborative learning framework for LD-COS. SCALER integrates the consistency regularization of the mean-teacher model with a learnable SAM for knowledge distillation and reciprocal adaptation. They are optimized alternately in two phases, with pseudo-label generation strategies tailored to their respective properties.

In **Phase I**, we train the segmenter within the meanteacher framework while keeping SAM fixed. Given the segmenter's sensitivity to label noise, we introduce an entropybased image-level weighting mechanism and an uncertaintybased pixel-level weighting strategy to selectively leverage pseudo-labels generated by both the teacher network and the fixed SAM. These strategies aim to suppress unreliable regions and reduce the influence of low-quality supervision. Besides, for samples that are already well-segmented by the segmenter, we apply strong augmentations to mine potentially informative features previously overlooked.

In **Phase II**, we fix the mean-teacher framework and use it to generate pseudo-labels for updating SAM. To exploit SAM's robustness to perturbations, we propose an augmentation invariance loss and a noise resistance loss. The augmentation invariance loss encourages SAM to maintain

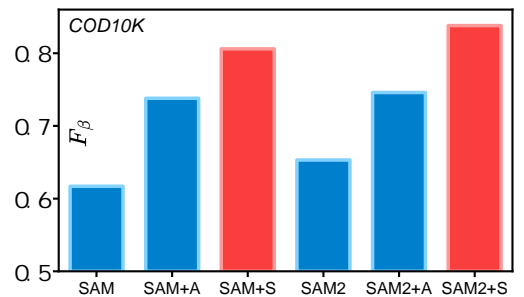


Figure 2. Quality of pseudo-labels from different SAM variants.

consistent predictions under weak and strong augmentations, facilitating robust representation learning without impairing generalization. The noise resistance loss enables SAM to utilize label-deficient data more effectively, even when pseudo-labels are noisy. By increasing the diversity and quantity of training samples, this strategy mitigates the overfitting that SAM may encounter under limited supervision.

By alternately optimizing the two phases, both the segmenter and SAM are progressively improved through mutual knowledge transfer. This iterative training scheme enables more effective utilization of label-deficient data, ultimately enhancing segmentation performance in COS tasks. Our contributions can be summarized as follows:

- We propose a novel bi-directional collaborative learning framework, SCALER, that enables a downstream segmenter and a SAM-based model to achieve mutual enhancement in LDCOS tasks. We demonstrate this mechanism is effective for both SSCOS and WSCOS settings.
- We design two specialized optimization phases that make this mutual learning possible. For the segmenter (Phase I), we introduce entropy- and uncertainty-based weighting strategies to filter noise from teacher pseudo-labels. For SAM (Phase II), we propose a novel augmentation invariance loss and noise resistance loss, allowing robust learning from the segmenter's noisy feedback.
- Extensive experiments on eight tasks validate our effectiveness and generalization, showing that our bi-directional SCALER outperforms prior one-way methods (WS-SAM and SEE) and successfully enhances the performance of vision foundation models like SAM and SAM2.

2. Related Work

Concealed Object Segmentation. Learning-based segmenters have achieved notable progress in COS under full supervision [6, 10, 12, 14]. Representative methods include SINet [6] for reversible segmentation, FEDER [10] for edge-assisted refinement, Camouflageator [12] for adversarial sample generation, and RUN [14] for model-driven optimization. Recent LDCOS techniques, including semi- and weakly-supervised setups, mainly employ consistency regularization [15, 20] or SAM-based pseudolabeling [11, 13, 16, 19]. However, unstable consistency

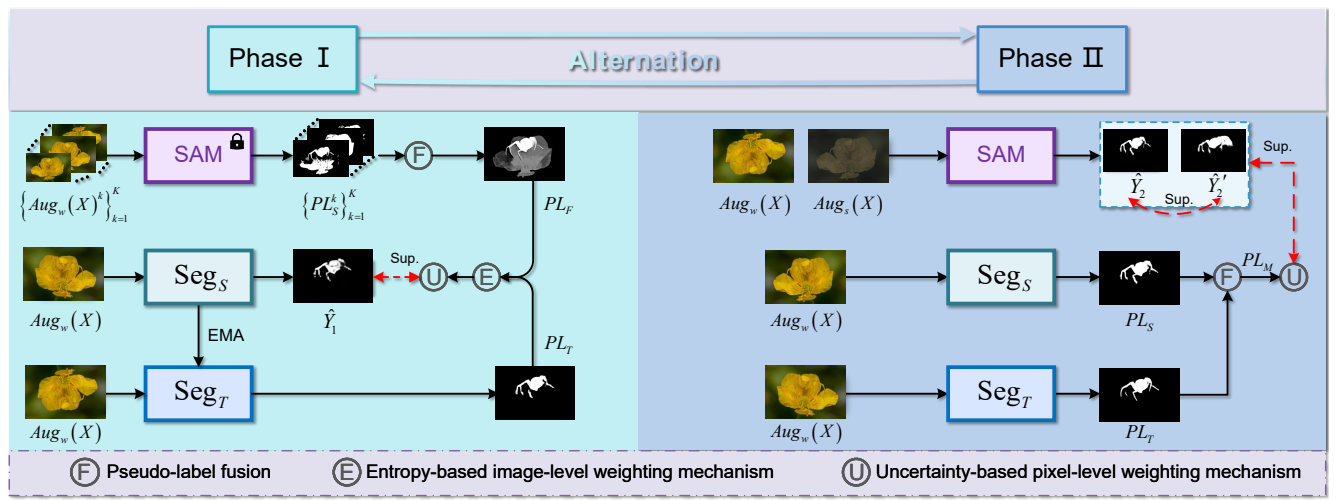


Figure 3. The bi-directional collaborative learning framework of SCALER. The framework alternates between two optimization phases, which enables the models to mutually enhance each other. Notably, our framework supports the integration of various existing segmenters and SAM/SAM2 fine-tuning approaches. Augmentation strategies are randomly sampled to further enhance training flexibility.

and task-agnostic SAM supervision often lead to suboptimal segmentation. To resolve this, SCALER unifies consistency regularization and adaptive SAM-based learning to achieve mutual refinement between the segmenter and the vision foundation model, promoting segmentation performance.

Label-Deficient Image Segmentation. Semi- and weaklysupervised segmentation improve label efficiency through regularization and pseudo-label refinement[1, 2, 21, 24]. A common paradigm is the teacher-student family, especially the mean-teacher framework[26], where a teacher updated by an exponential moving average (EMA) of the student provides temporally ensembled targets for consistency learning. However, in COS, the ambiguous boundaries and low contrast destabilize pseudo-labels and amplify error accumulation. Meanwhile, fixed or lightly tuned foundation models such as SAM [19] suffer domain gaps in concealed scenes. Recent methods, e.g., WS-SAM [11] and SEE [13], design complex pseudo-label filtering strategies to filter out valuable pseudo-labels generated by SAM, restricted by the limited capacity of SAM and suffering from limited training data. SCALER addresses these issues via alternating optimization: a mean-teacher module enforces robust consistency on the segmenter with uncertainty-aware weighting, while SAM is iteratively adapted with augmentation-invariance and noiseresistance losses. This collaborative design, unlike prior one-way distillation, enables bidirectional knowledge transfer and improves both specialized segmenters and foundation models in label-scarce scenarios.

3. Methodology

Label-deficient concealed object segmentation (LDCOS), including semi-supervised COS (SSCOS) and weakly supervised COS (WSCOS), aims to train a segmenter from a partially labeled training set $S = \{X_i, Y_i\}_{i=1}^{S}$ and evaluate

it on a test set $\mathcal{T} = \{T_i\}_{i=1}^T$, where X_i and T_i denote input images and Y_i denotes the corresponding deficient label. In SSCOS, Y_i is missing for some training samples, whereas in WSCOS, Y_i comprises sparse annotations (e.g., points or scribbles) marking foreground and background regions.

Training an LDCOS model is challenging for two reasons. First, pure consistency constraints can be unstable due to the concealed nature of targets. Second, while SAM [19] provides general priors, its predictions suffer from domain gaps. Prior methods [11, 13] address this through *one-way* knowledge transfer (from SAM to the segmenter) but lack a mechanism for the segmenter, which becomes a domain specialist, to reciprocally improve SAM.

To overcome this, we propose **SCALER**, a <u>SAM-Enhanced CollA</u>borative <u>LEaRning</u> framework that enables *bi-directional* knowledge exchange. As illustrated in Fig. 3, SCALER integrates a mean-teacher framework (for consistency) with a learnable SAM (for mutual distillation). The key innovation lies in alternating optimization across two phases: the segmenter learns from SAM (Phase I) while SAM learns from the specialized segmenter (Phase II), creating a mutually beneficial training loop.

3.1. Phase I: Training Segmenter with Fixed SAM

In Phase I, we fix SAM (as a static "generalist" teacher) and optimize the segmenter. This segmenter benefits from dual-source supervision: (1) consistency regularization from its own teacher model (Seg_T) and (2) general knowledge from the frozen SAM (can be any vision foundation model). **Dual pseudo-label generation**. We generate two primary pseudo-labels. First, for the teacher model Seg_T, we apply a random weak augmentation $Aug_w(\cdot)$ to each input X and obtain the initial pseudo-label PL_T , formulated as:

$$PL_T = \operatorname{Seg}_T \left(Aug_w(X) \right). \tag{1}$$

Next, for SAM, we generate K stochastic augmentations of X_i , $\{Aug_w(X)^k\}_{k=1}^K$, by randomly sampling flips, rotations $(0^\circ, 90^\circ, 180^\circ, 270^\circ)$, and scales $(\times 0.5, \times 1.0, \times 2.0)$. Feeding these variants into SAM yields pseudo-labels:

$$\{PL_S^k\}_{k=1}^K = \text{SAM}(\{Aug_w(X)^k\}_{k=1}^K).$$
 (2)

We then aggregate these masks by averaging:

$$PL_F = \frac{1}{K} \sum_{k=1}^{K} PL_S^k.$$
 (3)

This ensemble strategy leverages SAM's sensitivity to subtle variations [13], yielding a PL_F that is generally more accurate than any single prediction.

Pseudo-label refinement. Since initial pseudo-labels may be unreliable for some samples and pixel-level predictions, we propose two complementary weighting mechanisms: entropy-based image-level weighting and uncertainty-based pixel-level weighting. These mechanisms emphasize reliable regions within relatively easy-to-segment samples. Both strategies are applied to pseudo-labels generated by the teacher model and SAM, formulated as:

$$E(PL_T) = \frac{1}{N} \sum_{i}^{N} -PL_T^i \log_2 PL_T^i - (1 - PL_T^i) \log_2 (1 - PL_T^i),$$
 (4)

$$E(PL_F) = \frac{1}{N} \sum_{i}^{N} -PL_F^i \log_2 PL_F^i - (1 - PL_F^i) \log_2 (1 - PL_F^i),$$
 (5)

where N represents the number of pixels. This weighting reduces the influence of samples with high entropy, which indicates low confidence and potential to mislead the network. The uncertainty-based pixel-level weighting mechanisms are $U(PL_T) = (2PL_T - 1)^2$, $U(PL_F) = (2PL_F - 1)^2$, (6)

which attenuates pixels with predictions near 0.5, reflecting ambiguity in distinguishing foreground from background.

Unlike prior methods [11, 13] that simply combine these, we define a basic weighted loss $R_b(\cdot)$ and apply it piecewise based on sample difficulty. The basic loss $R_b(\cdot)$ combines sample confidence $(1 - E(\cdot))$ with pixel certainty $U(\cdot)$:

$$R_b(PL_T, \hat{Y}_1) = (1 - E(PL_T)) \cdot U(PL_T) \cdot (L_{ce}(\hat{Y}_1, PL_T) + L_{IoU}(\hat{Y}_1, PL_T)),$$
(7)

where $L_{ce}(\cdot)$ and $L_{IoU}(\cdot)$ correspond to the cross-entropy loss and the intersection-over-union loss, respectively. \hat{Y}_1 is the output of the student segmenter, defined as

$$\hat{Y}_1 = \operatorname{Seg}_S(Aug_w(X)). \tag{8}$$

We further address two extreme cases:

(1) Difficult samples: If the entropy $E(PL_T)$ is greater than or equal to 0.8, indicating low confidence, we introduce a mask w_{PL_T} to isolate trustworthy pixels:

$$w_{PL_T} = \begin{cases} 0 & PL_T \in [0.1, 0.9], \\ 1 & \text{Otherwise.} \end{cases}$$
 (9)

In this case, the refined pseudo-labels are defined as:

$$R(PL_T, \hat{Y}_1) = w_{PL_T} \cdot R_b(PL_T, \hat{Y}_1).$$
 (10)

(2) Simple samples: For samples where the entropy of

predictions $E(\hat{Y}_1)$ is less than or equal to 0.2, we apply additional strong augmentations $Aug_s(\cdot)$ to increase task difficulty, obtaining another prediction $\hat{Y}_1' = \mathrm{Seg}_S(Aug_s(X))$. The refinement strategy becomes:

 $R(PL_T, \hat{Y}_1) = R_b(PL_T, \hat{Y}_1) + R_b(PL_T, \hat{Y}'_1).$ (11) Overall, the piecewise refinement strategy is defined as:

$$R(PL_{T}, Y_{1}) = \begin{cases} w_{PL_{F}} \cdot R_{b}(PL_{T}, \hat{Y}_{1}), & E(PL_{T}) \ge 0.8, \\ R_{b}(PL_{T}, \hat{Y}_{1}) + R_{b}(PL_{T}, \hat{Y}'_{1}), & E(\hat{Y}_{1}) \le 0.2, \\ R_{b}(PL_{T}, \hat{Y}_{1}). & \text{Otherwise.} \end{cases}$$
(12)

Optimization. Under weak supervision, the segmenter is trained with the annotations Y and our refinement strategy:

$$\mathcal{L}_{w}^{1} = R(PL_{T}, \hat{Y}_{1}) + R(PL_{F}, \hat{Y}_{1}) + L_{pce}(Y, \hat{Y}_{1}), \quad (13)$$
 where \mathcal{L}_{pce} is the partial cross-entropy loss. Under semi-supervision, \mathcal{L}_{pce} is replaced by $\mathcal{L}_{ce} + \mathcal{L}_{IoU}$ for labeled samples, while unlabeled samples use the refinement loss:

$$\mathcal{L}_{s}^{1} = (R(PL_{T}, \hat{Y}_{1}) + R(PL_{F}, \hat{Y}_{1})) + (L_{ce}(Y, \hat{Y}_{1}) + L_{IoU}(Y, \hat{Y}_{1})).$$
(14)

The teacher weights θ_T are updated via an exponential moving average (EMA) strategy from the student θ_S :

$$\theta_t = \eta \theta_T + (1 - \eta)\theta_S$$
, with $\eta = 0.996$. (15)

3.2. Phase II: Optimizing SAM via Seg. Feedback

This phase enables the novel *bi-directional* learning. We reverse the roles: the specialized mean-teacher framework (Seg_S, Seg_T) is now *fixed* and serves as a "specialist" teacher to update the *learnable* SAM (via SAMadapter [3]).

This requires SAM (a generalist) to learn from a specialist's noisy pseudo-labels. We generate a consensus pseudo-label PL_M from the fixed segmenter framework, $PL_M = (PL_S + PL_T)/2$, where $PL_S = \mathrm{Seg}_S(Aug_w(X))$ and $PL_T = \mathrm{Seg}_T(Aug_w(X))$. We then design two losses to make this knowledge transfer robust.

Augmentation Invariance Loss (\mathcal{L}_{ai}). We exploit SAM's robustness by enforcing prediction consistency between weak and strong augmentations:

$$\mathcal{L}_{ai} = \mathcal{L}_{ce}(\hat{Y}_2, \hat{Y}_2') + \mathcal{L}_{IoU}(\hat{Y}_2, \hat{Y}_2'), \tag{16}$$

where $\hat{Y}_2 = \text{SAM}(Aug_w(X))$ and $\hat{Y}_2' = \text{SAM}(Aug_s(X))$. This loss function facilitates robust representation learning while not impairing generalization.

Noise Resistance Loss (\mathcal{L}_{nr}) . This loss distills knowledge from the segmenter's pseudo-label PL_M while protecting SAM from its noise. We apply the pixel-level uncertainty weight $U(\cdot)$ to ignore ambiguous pixels, but we omit the sample-level entropy weight $E(\cdot)$ to ensure SAM learns from all samples, even difficult ones. \mathcal{L}_{nr} is defined as:

$$\mathcal{L}_{nr} = U(PL_M) \cdot (\mathcal{L}_{ce}(\hat{Y}_2, PL_M) + \mathcal{L}_{IoU}(\hat{Y}_2, PL_M)),$$
 (17) The two loss functions, by increasing the diversity and quantity of training samples, jointly mitigate the overfitting that SAM may encounter under limited supervision.

Table 1. Results on COD of the WSCOS task with point supervision and scribble supervision. The best two results are in red and blue fonts.

	Pub.	1 .	CHAMELEON				CA	МО		COD10K				NC4K			
Methods		$M \downarrow$	$F_{\beta} \uparrow$	$E_{\phi} \uparrow$		$M \downarrow$		$E_{\phi} \uparrow$	$S_{\alpha} \uparrow$	$M\downarrow$	$F_{\beta} \uparrow$	$E_{\phi} \uparrow$	$S_{\alpha} \uparrow$	$M \downarrow$	$F_{\beta} \uparrow$		$S_{\alpha} \uparrow$
		<i>IVI</i> ↓	1'β	E_{ϕ}	\mathcal{O}_{α}	<i>IVI</i> ↓	Iβ	E_{ϕ}	ω_{α}	1VI ↓	Iβ	E_{ϕ}	\mathcal{O}_{α}	<i>1VI</i> ↓	1'β	E_{ϕ}	\mathcal{O}_{α}
						Scril	bble Su	pervisi	on								
SAM [19]	ICCV23	0.207	0.595	0.647	0.635	0.160	0.597	0.639	0.643	0.093	0.673	0.737	0.730	0.118	0.675	0.723	0.717
$SAM-W_S$ [3]	ICCVW23	0.069	0.751	0.835	0.661	0.097	0.696	0.788	0.738	0.049	0.712	0.833	0.770	0.066	0.757	0.842	0.768
WSSA [30]	CVPR20	0.067	0.692	0.860	0.782	0.118	0.615	0.786	0.696	0.071	0.536	0.770	0.684	0.091	0.657	0.779	0.761
SCWS [29]	AAAI21	0.053	0.758	0.881	0.792	0.102	0.658	0.795	0.713	0.055	0.602	0.805	0.710	0.073	0.723	0.814	0.784
TEL [22]	CVPR22	0.073	0.708	0.827	0.785	0.104	0.681	0.797	0.717	0.057	0.633	0.826	0.724	0.075	0.754	0.832	0.782
SCOD [15]	AAAI23	0.046	0.791	0.897	0.818	0.092	0.709	0.815	0.735	0.049	0.637	0.832	0.733	0.064	0.751	0.853	0.779
GenSAM [16]	AAAI24	0.090	0.680	0.807	0.764	0.113	0.659	0.775	0.719	0.067	0.681	0.838	0.775	0.097	0.687	0.750	0.732
WS-SAM [11]	NIPS23	0.046	0.777	0.897	0.824	0.092	0.742	0.818	0.759	0.038	0.719	0.878	0.803	0.052	0.802	0.886	0.829
SEE [13]	TPAMI25	0.044	0.785	0.903	0.826	0.090	0.747	0.826	0.765	0.036	0.729	0.883	0.807	0.051	0.808	0.891	0.836
SCALER (Ours)	_	0.042	0.788	0.912	0.838	0.089	0.785	0.834	0.778	0.034	0.736	0.882	0.815	0.050	0.809	0.897	0.817
						Po	int Sup	ervisio	n								
SAM [19]	ICCV23	0.207	0.595	0.647	0.635	0.160	0.597	0.639	0.643	0.093	0.673	0.737	0.730	0.118	0.675	0.723	0.717
$SAM-W_P[3]$	ICCVW23	0.095	0.708	0.752	0.688	0.117	0.653	0.698	0.681	0.068	0.697	0.805	0.767	0.078	0.736	0.793	0.782
WSSA [30]	CVPR20	0.105	0.660	0.712	0.711	0.148	0.607	0.652	0.649	0.087	0.509	0.733	0.642	0.104	0.688	0.756	0.743
SCWS [29]	AAAI21	0.097	0.684	0.739	0.714	0.142	0.624	0.672	0.687	0.082	0.593	0.777	0.738	0.098	0.695	0.767	0.754
TEL [22]	CVPR22	0.094	0.712	0.751	0.746	0.133	0.662	0.674	0.645	0.063	0.623	0.803	0.727	0.085	0.725	0.795	0.766
SCOD [15]	AAAI23	0.092	0.688	0.746	0.725	0.137	0.629	0.688	0.663	0.060	0.607	0.802	0.711	0.080	0.744	0.796	0.758
GenSAM [16]	AAAI24	0.090	0.680	0.807	0.764	0.113	0.659	0.775	0.719	0.067	0.681	0.838	0.775	0.097	0.687	0.750	0.732
WS-SAM [11]	NIPS23	0.056	0.767	0.868	0.805	0.102	0.703	0.757	0.718	0.039	0.698	0.856	0.790	0.057	0.801	0.859	0.813
SEE [13]	TPAMI25	0.055	0.772	0.872	0.806	0.098	0.712	0.769	0.721	0.038	0.706	0.862	0.796	0.055	0.806	0.867	0.817
SCALER (Ours)		0.054	0.779	0.869	0.809	0.096	0.716	0.779	0.729	0.039	0.718	0.879	0.802	0.054	0.809	0.863	0.821

Optimization. SAM, with weak supervision, is updated via

$$\mathcal{L}_w^2 = \mathcal{L}_{ai} + \mathcal{L}_{nr} + \mathcal{L}_{pce}(Y, \hat{Y}_2). \tag{18}$$

Under semi-supervision, the loss \mathcal{L}^2_s combines this with a standard supervised loss on labeled data, formulated as

$$\mathcal{L}_{s}^{2} = [\mathcal{L}_{ai} + \mathcal{L}_{nr}] + [\mathcal{L}_{ce}(Y, \hat{Y}_{2}) + \mathcal{L}_{IoU}(Y, \hat{Y}_{2})]. \quad (19)$$

3.3. Optimization Procedure

The full SCALER pipeline proceeds in three stages to ensure stable convergence toward mutual enhancement.

- (1) Stage 1 (Initialization): We first pretrain the meanteacher framework and fine-tune SAM separately using only the available labeled COS data. This provides both models with a strong, task-specific starting point.
- (2) Stage 2 (Segmenter Warm-up): We fix the initialized SAM and run only Phase I on the full label-deficient dataset. This allows the segmenter to quickly develop strong specialization by leveraging SAM's generalist pseudo-labels.
- (3) Stage 3 (Iterative Mutual Enhancement): This is the core. We alternately optimize Phase I (enhancing the segmenter with SAM) and Phase II (enhancing SAM via the segmenter). Each model generates pseudo-labels that fit their corresponding characteristic for the other, facilitating the iterative mutual enhancement described in our contributions.

4. Experiments

4.1. Experimental Setup

Implementation details. We implement our method in Py-Torch using two RTX 6000 Ada GPUs. Following [11], we adopt ResNet50 pre-trained on ImageNet [5] as the default backbone. All input images are resized to 352×352 for both training and testing. The Adam optimizer is used for training, with momentum parameters set to (0.9, 0.999). The batch size is fixed at 12, and the initial learning rate is set to 0.0001, which is reduced by a factor of 0.1 every 80 epochs. The number of augmentation images K is set to 12. In this paper, our segmenter is the same as WS-SAM [11] for fairness. We fine-tune SAM using SAM-Adapter [3], but other adaptation strategies and foundation models (e.g., SAM2) can be seamlessly integrated into SCALER. In general, stronger foundation models and/or more effective fine-tuning strategies provide higher-quality pseudo-labels, yielding further gains for the segmenter and, via Phase II, additional improvements for the foundation model itself.

4.2. Comparative Evaluation

Following [11], we report results with point annotations under weak supervision. For the COD task, we further assess performance with scribble annotations provided by [8].

Camouflaged object detection. Tables 1 and 2 show that our SCALER framework outperforms competing methods in both weakly supervised and semi-supervised settings. Although fine-tuning SAM via SAMadapter [3] under point

Table 2. Results on COD of the SSCOS task with 1/8 and 1/16 labeled training data.

	Table 2. Results on COD of the SSCOS task with 1/8 and 1/10 labeled training data. CHAMELEON CAMO COD10K											NC	C4K				
Methods	Pub.					$M\downarrow$			$S_{\alpha} \uparrow$	$M\downarrow$			$S_{\alpha} \uparrow$	$M \downarrow$		$E_{\phi} \uparrow$	$S_{\alpha} \uparrow$
		,		7 1		1/8 Lat				,		7 '		,	, ,	7 ,	
SAM [19]	ICCV23	0.207	0.595	0.647		0.160				0.093	0.673	0.737	0.730	0.118	0.675	0.723	0.717
SAM-S [3]	ICCVW23	1	0.667							1	0.695			1		0.756	
DTEN [24]	CVPR23					0.103					0.635					0.833	
PGCL [1]	CVPR23					0.096											
EPS [21] CoSOD [2]	TPAMI23 WACV24	ı				0.090 0.092				1						0.855	
SEE [13]	TPAMI25					0.092											
SCALER (Ours)	_					0.081											
		ı				1/16 La	beled T	raining	Data	1							
SAM [19]	ICCV23	0.207	0.595	0.647		0.160				0.093	0.673	0.737	0.730	0.118	0.675	0.723	0.717
SAM-S [3]	ICCVW23					0.146											
DTEN [24]	CVPR23	l				0.123				1				1			
PGCL [1]	CVPR23	l				0.116				1				1			
EPS [21] CoSOD [2]	TPAMI23 WACV24					0.103 0.099											
SEE [13]	TPAMI25					0.099											
SCALER (Ours)	—					0.091											
COD				1.		13	1)	7	ber		•	1	7			1
						<u>U</u>	¥		Q			- No.	•			N. F.	
PS S						_				5						N. Contract of the Contract of	
								-					•				
							_			_[Ł	-
					`												
TOD												,					1
		1			7						1	7			1		
(a) Origin	(b) G	T		CALE		(d) S			VS-SA		f) Gen		(g)	SCOD) (ł	n) SAN	∕I-W P
			Figure	e 4. Vis	sualiza	tions fo	or COS	tasks	with po	oint sui	pervisio	on.					

Figure 4. Visualizations for COS tasks with point supervision.

 $(SAM-W_P)$, scribble $(SAM-W_S)$, and semi-supervised configurations yields performance improvements, these variants still underperform relative to SCALER. Furthermore,

SCALER surpasses the previously proposed WS-SAM [11] and SEE [13] frameworks across all evaluation protocols, demonstrating its effectiveness in producing higher-quality

Table 3. Results on PIS and TOD of the WSCOS task with point supervision.

					yp Ima			tion (P	IS)							Objec	t Detec			
Methods	CV	C-Ca	olonDE	3		ET	IS			Kva	ısir			GI)D			G°	SD	
	$M \downarrow F$	$r_{\beta} \uparrow$	$E_{\phi} \uparrow$	$S_{\alpha} \uparrow $	$M\downarrow$	$F_{\beta} \uparrow$	$E_{\phi} \uparrow$	$S_{\alpha} \uparrow$	$M\downarrow$	$F_{\beta} \uparrow$	$E_{\phi} \uparrow$	$S_{\alpha} \uparrow$	$M \downarrow$	$F_{\beta} \uparrow$	$E_{\phi} \uparrow$	$S_{\alpha} \uparrow$	$M\downarrow$	$F_{\beta} \uparrow$	$E_{\phi} \uparrow$	$S_{\alpha} \uparrow$
SAM [19]	0.479 0.	343	0.419	0.427	0.429	0.439	0.512	0.503	0.320	0.545	0.564	0.582	0.245	0.512	0.530	0.551	0.266	0.473	0.501	0.514
$SAM-W_P[3]$	0.146 0.	612	0.690	0.683	0.125	0.650	0.731	0.728	0.093	0.818	0.823	0.815	0.143	0.691	0.733	0.636	0.137	0.715	0.752	0.681
WSSA [30]	0.127 0.0	645	0.732	0.713	0.123	0.647	0.733	0.762	0.082	0.822	0.852	0.828	0.173	0.652	0.710	0.616	0.185	0.661	0.712	0.650
SCWS [29]	0.082 0.0	674	0.758	0.787	0.085	0.646	0.768	0.731	0.078	0.837	0.860	0.831	0.170	0.631	0.702	0.613	0.172	0.706	0.738	0.673
TEL [22]	0.089 0.0	669	0.743	0.761	0.083	0.639	0.776	0.726	0.091	0.810	0.826	0.804	0.230	0.640	0.586	0.536	0.275	0.571	0.501	0.495
SCOD [15]	0.077 0.0	691	0.795	0.802	0.071	0.664	0.802	0.766	0.071	0.853	0.877	0.836	0.146	0.801	0.778	0.723	0.154	0.743	0.751	0.710
GenSAM [16]	0.079 0.0	665	0.739	0.793	0.073	0.665	0.813	0.772	0.073	0.841	0.866	0.829	0.115	0.712	0.795	0.737	0.127	0.757	0.760	0.724
WS-SAM [11]	0.043 0.	721	0.839	0.816	0.037	0.694	0.849	0.797	0.046	0.878	0.917	0.877	0.078	0.858	0.863	0.775	0.089	0.839	0.841	0.764
SEE [13]	0.042 0.	726	0.842	0.819	0.035	0.705	0.857	0.800	0.045	0.883	0.918	0.879	0.073	0.867	0.871	0.777	0.081	0.846	0.849	0.768
SCALER (Ours)	0.042 0.	731	0.844	0.822	0.036	0.708	0.861	0.802	0.044	0.895	0.917	0.883	0.072	0.871	0.871	0.779	0.083	0.849	0.853	0.768
Table 4. Results on PIS and TOD of the SSCOS task.																				
				Po	lyp Im	age Se	gmenta	ation (F	PIS)					Tran	ısparen	t Objec	ct Detection (TOD)			
Methods	CVC-ColonDB ETIS						TIS	Kvasir					GDD				GSD			
	$M \downarrow H$	$F_{\beta} \uparrow$	$E_{\phi} \uparrow$	$S_{\alpha} \uparrow$	$M \downarrow$	$F_{\beta} \uparrow$	$E_{\phi} \uparrow$	$S_{\alpha} \uparrow$	$M \downarrow$	$F_{\beta} \uparrow$	$E_{\phi} \uparrow$	$S_{\alpha} \uparrow$	$M \downarrow$	$F_{\beta} \uparrow$	$E_{\phi} \uparrow$	$S_{\alpha} \uparrow$	$M \downarrow$	$F_{\beta} \uparrow$	$E_{\phi} \uparrow$	$S_{\alpha} \uparrow$
1/8 Labeled Training Data																				
SAM [19]	0.479 0	.343	0.419	0.427	0.429	0.439	0.512	0.503	0.320	0.545	0.564	0.582	0.245	0.512	0.530	0.551	0.266	0.473	0.501	0.514
SAM-S [3]	0.185 0	.517	0.627	0.661	0.172	0.558	0.706	0.682	0.131	0.738	0.772	0.783	0.185	0.674	0.703	0.618	0.177	0.688	0.724	0.652
DTEN [24]	0.073 0	.607	0.722	0.743	0.064	0.607	0.759	0.757	0.078	0.837	0.867	0.833	0.096	0.815	0.818	0.733	0.102	0.803	0.792	0.736
PGCL [1]	0.068 0	.629	0.743	0.749	0.057	0.623	0.771	0.764	0.070	0.838	0.869	0.855	0.097	0.819	0.823	0.747	0.095	0.817	0.804	0.741
EPS [21]	0.060 0	.645	0.758	0.756	0.053	0.642	0.786	0.772	0.063	0.847	0.883	0.858	0.085	0.837	0.842	0.759	0.089	0.829	0.817	0.754
CoSOD [2]	0.057 0	.657	0.776	0.763	0.047	0.639	0.802	0.780	0.056	0.859	0.886	0.863	0.088	0.831	0.835	0.756	0.091	0.826	0.813	0.749
SEE [13]	0.045 0	.706	0.828	0.801	0.039	0.692	0.832	0.792	0.051	0.867	0.905	0.869	0.076	0.846	0.855	0.768	0.085	0.835	0.832	0.763
SCALER (Ours)	0.043 0	.726	0.841	0.823	0.038	0.685	0.851	0.798	0.050	0.873	0.914	0.879	0.073	0.854	0.849	0.781	0.083	0.845	0.841	0.777
							1/	16 Lab	eled T	raining	Data									
SAM [19]	0.479 0	.343	0.419	0.427	0.429	0.439	0.512	0.503	0.320	0.545	0.564	0.582	0.245	0.512	0.530	0.551	0.266	0.473	0.501	0.514
SAM-S [3]	0.201 0								1				1							
DTEN [24]	0.080 0	.586	0.696	0.732	0.071	0.592	0.730	0.750	0.086	0.813	0.824	0.833	0.112	0.797	0.810	0.736	0.115	0.786	0.770	0.705
PGCL [1]	0.075 0								1				1							
EPS [21]	0.065 0				1				1								1			
CoSOD [2]	0.063 0	.638	0.754	0.755	0.050	0.632	0.781	0.767	0.066	0.840	0.871	0.852	0.095	0.813	0.816	0.746	0.105	0.793	0.792	0.732
SEE (Ours)	0.050 0								1				1							
SCALER (Ours)	0.048 0	.698	0.821	0.777	0.041	0.686	0.822	0.799	0.056	0.878	0.899	0.885	0.078	0.851	0.848	0.767	0.082	0.819	0.831	0.768

pseudo-labels. Fig. 4 provides qualitative comparisons under point supervision, further illustrating the advantages of our alternating optimization strategy.

Polyp image segmentation. Polyps often exhibit strong visual similarity to surrounding tissue, making polyp image segmentation (PIS) particularly challenging. As shown in Tables 3 and 4, our SCALER framework significantly outperforms the next best method, SEE, under point supervision. Both SAM and SAM-W $_{\rm P}$ perform poorly on this task, underscoring their limitations in handling concealed polyps. Fig. 4 illustrates that our approach more accurately localizes hidden polyps and produces segmentation boundaries that closely match the true lesion contours.

Transparent object detection. TOD is essential for enhancing vision systems in robotics, yet it remains challenging due to the minimal visual contrast of objects. As shown in Tables 3 and 4, our SCALER framework surpasses current state-of-the-art methods under both weakly and semi-supervised settings. Fig. 4 illustrates that our method not

only localizes transparent objects with high accuracy but also refines their segmentation boundaries and effectively suppresses background clutter.

4.3. Ablation Study

Experiments are conducted on the *COD10K* dataset with scribble supervision in Secs. 4.3 and 4.4.

Effectiveness in Phase I. As shown in Tab. 5, in Phase I, we observe performance degradation upon removing the fused pseudo-label PL_F , the entropy-based image-level weighting mechanism $E(\cdot)$, or the uncertainty-based pixel-level weighting mechanism $U(\cdot)$. Besides, omitting our specialized refinement procedures for difficult samples (denoted $R_1(\cdot)$) and simple samples (denoted $R_2(\cdot)$) also leads to a noticeable performance drop. These results demonstrate the effectiveness of our strategies.

Effectiveness in Phase II. As shown in Tab. 5, removing Phase II entirely (*i.e.*, running only Stage 1 and 2) reverts SCALER to a one-way framework. This "w/o Phase II" ab-

Table 5. Ablation study in the COD task on the COD10K dataset with the scribble supervision.

Metrics			Phas					Phase II	Optin	SCALER			
Wictires	w/o PL_F	w/o $E(\cdot)$	w/o $U(\cdot)$	$R_1(\bullet) \to R(\bullet)$	$R_2(\bullet) \to R(\bullet)$	w/o Phase	II w/o \mathcal{L}_{ai}	$\mathcal{L}^1_{ai} o \mathcal{L}_{ai}$	w/o \mathcal{L}_{nr}	$\mathcal{L}_{nr}^1 o \mathcal{L}_{nr}$	w/o step 1	w/o step 2	(Ours)
$M \downarrow$	0.039	0.036	0.038	0.037	0.035	0.037	0.036	0.039	0.036	0.035	0.040	0.036	0.034
$F_{\beta}\uparrow$	0.732	0.724	0.721	0.728	0.722	0.723	0.733	0.730	0.729	0.734	0.720	0.733	0.736
$E_{\phi} \uparrow$	0.863	0.870	0.869	0.866	0.868	0.860	0.865	0.869	0.870	0.879	0.864	0.875	0.882
$S_{lpha}\uparrow$	0.804	0.805	0.813	0.806	0.808	0.805	0.812	0.804	0.807	0.809	0.802	0.811	0.815

Table 6. Generalization of SCALER. "+" means integrating Table 7. Performance of foundation models with different training manners, the method with our SCALER framework. Our SCALER "SAM" and "SAM2" are trained under our SCALER framework, while the serves as a plug-and-play framework for existing methods. two "adapters" indicate direct fine-tuning of the foundation models.

Metrics	GenSAM	GenSAM+	WS-SAM	WS-SAM+	SEE	SEE+	Metrics	SCALER+S	SAM	SAMadapter [3]	SCALER+S2	SAM2	SAM2adapter [4]
$M \downarrow$	0.067	0.061	0.038	0.036	0.036	0.035	$M \downarrow$	0.034	0.027	0.036	0.033	0.023	0.035
$F_{\beta} \uparrow$	0.681	0.693	0.719	0.728	0.729	0.738	$F_{\beta} \uparrow$	0.736	0.765	0.732	0.741	0.778	0.733
$E_{\phi} \uparrow$	0.838	0.851	0.878	0.887	0.883	0.886	$E_{\phi} \uparrow$	0.882	0.912	0.888	0.889	0.920	0.886
$S_{\alpha} \uparrow$	0.775	0.780	0.803	0.809	0.807	0.813	$S_{\alpha} \uparrow$	0.815	0.831	0.818	0.819	0.835	0.820

lation shows a significant performance drop, confirming that the mutual enhancement from Phase II is critical. We further evaluate the proposed augmentation invariance loss L_{ai} and noise resistance loss L_{nr} . Specifically, using an alternative L_{ai}^1 , which imposes invariance between two weak augmentations only, or employing L_{nr}^1 , which directly applies the refinement strategy $R(\cdot)$ from Phase I, results in decreased performance. This confirms that our proposed loss functions are better tailored for effectively fine-tuning SAM.

Impact of the optimization procedure. To enhance the capability of both SAM and the mean-teacher framework in generating high-quality pseudo-labels, we structure our optimization procedure into three sequential steps, with the initial two steps dedicated to network pretraining. As indicated in Tab. 5, each of these pretraining steps contributes positively to the overall segmentation performance, underscoring their importance in our proposed method.

4.4. Further Analysis

Results on salient object detection are placed in the Supp. **Generalizability of our SCALER**. As shown in Tab. 7, integrating SCALER with cutting-edge methods (indicated by the suffix "+") yields performance gains. This demonstrates the potential of SCALER to function as a plug-and-play framework for enhancing existing segmentation models.

Performance of foundation models with different training manners. As shown in Tab. 7, foundation models trained within our SCALER framework achieve substantially better performance than those directly fine-tuned with adapter-based methods. We also report results of our segmenter using SAM and SAM2 as the foundation models, denoted as "+S" and "+S2" respectively. Notably, our segmenter even surpasses the large foundation models fine-tuned via adapters, demonstrating the effectiveness and superiority of the proposed bi-directional collaborative learning framework.

5. Discussions

Beyond proposing a robust LDCOS framework, SCALER reveals an important insight from its bi-directional design: a lightweight, task-specific segmenter can effectively guide a large, generalist foundation model—such as SAM—under

label-deficient conditions. This finding underscores the advantage of mutual knowledge transfer over the one-way distillation used in previous works[11, 13]. By enabling the foundation model to benefit from the segmenter's domain specialization, SCALER improves adaptation in challenging settings (e.g., medical imaging)[17, 18, 23], suggesting a broader paradigm where knowledge is exchanged reciprocally rather than unidirectionally.

6. Limitations and Future Work

SCALER still has two main limitations. First, when both the segmenter and SAM simultaneously fail to localize an object, the mutual learning loop cannot start effectively. Future work will explore introducing auxiliary knowledge such as text prompts or generative priors to provide initial guidance and overcome this cold-start issue. Second, the proposed bi-directional learning paradigm, where a lightweight, task-specific model and a large foundation model mutually enhance each other, has broader potential. We plan to extend this principle to other label-deficient vision tasks, including object detection and depth estimation.

7. Conclusions

We propose SCALER, a unified framework for LDCOS, combining a mean-teacher approach for consistency regularization with a learnable SAM-based model for knowledge distillation. In Phase I, with SAM fixed, we refine the segmenter using image-level and pixel-level weighting schemes that select trustworthy regions in pseudo-labels. In Phase II, with the segmenter fixed, we update SAM by introducing an augmentation invariance loss and a noise resistance loss, promoting stable representation learning.

References

- [1] Hritam Basak and Zhaozheng Yin. Pseudo-label guided contrastive learning for semi-supervised medical image segmentation. In *CVPR*, pages 19786–19797, 2023. 3, 6, 7
- [2] Souradeep Chakraborty, Shujon Naha, Muhammet Bastan, Dimitris Samaras, et al. Unsupervised and semi-supervised co-salient object detection via segmentation frequency statistics. In *WACV*, pages 332–342, 2024. 3, 6, 7
- [3] Tianrun Chen, Lanyun Zhu, Chaotao Deng, Runlong Cao, Yan Wang, and Shangzhan Zhang. Sam-adapter: Adapting segment anything in underperformed scenes. In *ICCV*, pages 3367–3375, 2023. 4, 5, 6, 7, 8
- [4] Tianrun Chen, Ankang Lu, Lanyun Zhu, Chaotao Ding, Chunan Yu, Deyi Ji, Zejian Li, Lingyun Sun, Papa Mao, and Ying Zang. Sam2-adapter: Evaluating & adapting segment anything 2 in downstream tasks: Camouflage, shadow, medical image segmentation, and more. arXiv preprint arXiv:2408.04579, 2024. 8
- [5] Jia Deng, Wei Dong, Richard Socher, Li-Jia Li, and Kai Li. Imagenet: A large-scale hierarchical image database. In CVPR, pages 248–255, 2009. 5
- [6] Deng-Ping Fan, Ge-Peng Ji, Guolei Sun, Ming-Ming Cheng, and Jianbing Shen. Camouflaged object detection. In CVPR, pages 2777–2787, 2020. 1, 2
- [7] Deng-Ping Fan, Ge-Peng Ji, and Tao Zhou. Pranet: Parallel reverse attention network for polyp segmentation. In *MICCAI*, pages 263–273, 2020. 1
- [8] Shuyong Gao, Wei Zhang, Yan Wang, Qianyu Guo, Chenglong Zhang, Yangji He, and Wenqiang Zhang. Weakly-supervised salient object detection using point supervison. In AAAI, pages 670–678, 2022. 5
- [9] Chunming He, Kai Li, Guoxia Xu, Jiangpeng Yan, Longxiang Tang, and Yulun Zhang. Hqg-net: Unpaired medical image enhancement with high-quality guidance. *IEEE Trans. Neural Networks Learn. Syst.*, 2023. 1
- [10] Chunming He, Kai Li, Yachao Zhang, Longxiang Tang, and Yulun Zhang. Camouflaged object detection with feature decomposition and edge reconstruction. In CVPR, pages 22046–22055, 2023. 1, 2
- [11] Chunming He, Kai Li, Yachao Zhang, Guoxia Xu, and Longxiang Tang. Weakly-supervised concealed object segmentation with sam-based pseudo labeling and multi-scale feature grouping. *NeurIPS*, 2024. 1, 2, 3, 4, 5, 6, 7, 8
- [12] Chunming He, Kai Li, Yachao Zhang, Yulun Zhang, Zhenhua Guo, and Xiu Li. Strategic preys make acute predators: Enhancing camouflaged object detectors by generating camouflaged objects. *ICLR*, 2024. 2
- [13] Chunming He, Kai Li, Yachao Zhang, Ziyun Yang, Youwei Pang, Longxiang Tang, Chengyu Fang, Yulun Zhang, Linghe Kong, Xiu Li, and Sina Farsiu. Segment concealed objects with incomplete supervision. *IEEE Trans. Pattern Anal. Mach. Intell.*, 2025. 1, 2, 3, 4, 5, 6, 7, 8
- [14] Chunming He, Rihan Zhang, Fengyang Xiao, Chenyu Fang, Longxiang Tang, and Yulun Zhang. Run: Reversible unfolding network for concealed object segmentation. *ICML*, 2025. 1, 2

- [15] Ruozhen He, Qihua Dong, and Jiaying Lin. Weaklysupervised camouflaged object detection with scribble. AAAI, 2023. 1, 2, 5, 7
- [16] Jian Hu, Jiayi Lin, and Shaogang Gong. Relax image-specific prompt requirement in sam: A single generic prompt for segmenting camouflaged objects. In AAAI, pages 12511– 12518, 2024. 2, 5, 7
- [17] Ge-Peng Ji, Deng-Ping Fan, Peng Xu, Ming-Ming Cheng, and Bowen Zhou. Sam struggles in concealed scenes". arXiv preprint arXiv:2304.06022, 2023. 8
- [18] Wei Ji, Jingjing Li, Qi Bi, Wenbo Li, and Li Cheng. Segment anything is not always perfect: An investigation of sam on different real-world applications. arXiv preprint arXiv:2304.05750, 2023. 8
- [19] Alexander Kirillov, Eric Mintun, Nikhila Ravi, and Hanzi Mao. Segment anything. arXiv preprint arXiv:2304.02643, 2023. 2, 3, 5, 6, 7
- [20] Xunfa Lai, Zhiyu Yang, Jie Hu, Shengchuan Zhang, and Liujuan Cao. Camoteacher: Dual-rotation consistency learning for semi-supervised camouflaged object detection. arXiv preprint arXiv:2408.08050, 2024. 2
- [21] Minhyun Lee, Seungho Lee, Jongwuk Lee, and Hyunjung Shim. Saliency as pseudo-pixel supervision for weakly and semi-supervised semantic segmentation. *IEEE Trans. Pattern Anal. Mach. Intell.*, 45(10):12341–12357, 2023. 3, 6, 7
- [22] Zhiyuan Liang, Tiancai Wang, Xiangyu Zhang, Jian Sun, and Jianbing Shen. Tree energy loss: Towards sparsely annotated semantic segmentation. In CVPR, pages 16907–16916, 2022.
 5, 7
- [23] Maciej A Mazurowski, Haoyu Dong, Hanxue Gu, Jichen Yang, Nicholas Konz, and Yixin Zhang. Segment anything model for medical image analysis: an experimental study. arXiv preprint arXiv:2304.10517, 2023. 8
- [24] Guangyu Ren, Michalis Lazarou, Jing Yuan, and Tania Stathaki. Towards automated polyp segmentation using weakly-and semi-supervised learning and deformable transformers. In *CVPR*, pages 4355–4364, 2023. 3, 6, 7
- [25] Yanguang Sun, Chunyan Xu, Jian Yang, Hanyu Xuan, and Lei Luo. Frequency-spatial entanglement learning for camouflaged object detection. In ECCV, pages 343–360, 2024.
- [26] Antti Tarvainen and Harri Valpola. Mean teachers are better role models: Weight-averaged consistency targets improve semi-supervised deep learning results. *NeurIPS*, 30, 2017. 3
- [27] Fengyang Xiao, Pan Zhang, and Chunming He. Concealed object segmentation with hierarchical coherence modeling. In CAAI ICAI, pages 16–27, 2023. 1
- [28] Fengyang Xiao, Sujie Hu, Yuqi Shen, and Chunming He. A survey of camouflaged object detection and beyond. CAAI AIR, 2024.
- [29] Siyue Yu, Bingfeng Zhang, Jimin Xiao, and Eng Gee Lim. Structure-consistent weakly supervised salient object detection with local saliency coherence. In AAAI, pages 3234–3242, 2021. 5, 7
- [30] Jing Zhang, Xin Yu, Aixuan Li, Peipei Song, and Bowen Liu. Weakly-supervised salient object detection via scribble. In *CVPR*, pages 12546–12555, 2020. 5, 7

[31] Jianwei Zhao, Xin Li, Fan Yang, Qiang Zhai, Ao Luo, Zicheng Jiao, and Hong Cheng. Focusdiffuser: Perceiving local disparities for camouflaged object detection. In *ECCV*, pages 181–198, 2024. 2